Available online at www.sciencedirect.com
SCIENCE DIRECT
Polymer 47 (2006) 2069–2079
polymer
www.elsevier.com/locate/polymer

Segmental orientation of thermoplastic polyurethanes investigated by ^{1}H double-quantum NMR. Correlation with thermodynamic and mechanical properties

Alexandra Voda [a,b,*], Mihai A. Voda [b], Klaus Beck [a], Thomas Schauber [a], Matthias Adler [a], Thomas Dabisch [c], Martin Bescher [a], Michael Viol [d], Dan E. Demco [b,**], Bernhard Blümich [b]

[a] *Freudenberg Forschungsdienste KG, Weinheim D-69465, Germany*
[b] *Institut für Technische Chemie und Makromolekulare Chemie, Rheinisch-Westfälische Technische Hochschule, Worringerweg 1, Aachen D-52056, Germany*
[c] *Merkel Freudenberg Fluidtechnic GmbH, Schwalmstadt D-34613, Germany*
[d] *Freudenberg Dichtungs- und Schwingungstechnik, Weinheim D-69465, Germany*

Received 26 November 2005; received in revised form 2 January 2006; accepted 11 January 2006
Available online 2 February 2006

Abstract

The segmental orientation of a series of thermoplastic polyurethane (TPU) samples with different content in hard segments and different number average molecular weights of soft segments was investigated by ^{1}H double-quantum (DQ) NMR. The residual dipolar couplings of the hard segments were measured via the residual second van Vleck moments. A simple theoretical approach based on Rouse modes was developed to explain the orientation dependence of the hard segments on the number average molecular weight of the soft segments. The effective transverse relaxation rates of the hard segments were correlated to the ^{1}H residual dipolar couplings. Moreover, the correlation between the segmental orientation of the hard segments and the thermodynamic and mechanical properties of the TPU samples is investigated. The glass transition temperatures of the soft segments represent the relevant thermodynamic quantities. The mechanical parameters used for discussing the correlations are Young's modulus, yield stress, and rebound resilience angles from tensile testing and rebound resilience measurements.

Keywords: Thermoplastic polyurethane; ^{1}H double-quantum NMR; Residual dipolar couplings

1. Introduction

Segmental orientation measured by ^{1}H residual dipolar interactions provides information about the structure and molecular dynamics in elastomer materials [1–3] (and references therein). Structure–dynamics relationship can be investigated via changes induced in the residual dipolar couplings by cross-link density, the presence of fillers, the action of mechanical deformation forces, and the adsorption of small penetrant molecules. The difficulties related to these measurements are due to the small values of the residual spin couplings, the many-body character of the dipolar couplings and the presence of molecular motions, which, in some cases produces a supplementary encoding of the spin system response.

In the last years ^{1}H residual dipolar couplings were measured by different one- and two-dimensional NMR techniques [1–3] (and references therein). One approach to access to the residual dipolar couplings and dynamic order parameters model-free uses homonuclear and heteronuclear multiple-quantum (MQ) build-up [4–10] and decay [11] curves. These MQ efficiency curves measured in the initial regime of the excitation/reconversion periods give access to specific residual van Vleck moments [7]. The MQ-NMR measurements can be performed in low magnetic fields [7,10] and even in the presence of strongly inhomogeneous static and radio-frequency magnetic fields [11,12].

One important class of elastomers is that of thermoplastic polyurethanes (TPU). They combine the processability of thermoplastics with rubber-like elastic properties. In most cases, segmented TPUs are regarded as multi-block copolymers of the $(AB)_n$ type, where A and B represent repeat units of

* Corresponding authors. Tel.: +49 6201 804307; fax: +49 6201 805191.
** Tel.: +49 241 8026433; fax: +49 241 8022185.
E-mail addresses: alexandra.voda@freudenberg.de (A. Voda), demco@mc.rwth-aachen.de (D.E. Demco).

0032-3861/$ - see front matter © 2006 Elsevier Ltd. All rights reserved.
doi:10.1016/j.polymer.2006.01.023

the hard and soft segments. The hard segments (HS) are responsible for the dimensional stability of the TPU product, by providing physical cross-links through hydrogen bonds and act as reinforcing filler to the soft segments (SS), which are responsible for the flexibility of the TPU materials.

In the last years, the microscopic properties of thermoplastic elastomers were investigated by solid-state NMR [13–18]. Litvinov et al. [13] investigated multi-block (poly-(butylenes-therephtalate) block poly-(tetramethylene-oxide) (PTMO)) copolymers by ^{1}H NMR and ^{13}C NMR relaxation experiments. They proved that at room temperature three different phases coexist and the phase diagrams as well as the crystallinity of PBT were determined. Bertmer et al. [14] reported information about segmental mobility on the same systems using static ^{1}H double-quantum (DQ) NMR experiments in combination with homo- and heteronuclear dipolar filters. Recently, proton NMR transverse magnetization relaxation, differential scanning calorimetry (DSC), and rebound resilience (RR) techniques were used to characterize molecular chain mobility, phase composition, glass transition temperatures, and angles of rebound for a series of TPU samples [18]. The same set of samples was used in the present study.

The aim of this work is to report the segmental orientation for a series of TPU samples with different content in hard segments and different number average molecular weight of the soft segments. The segmental orientation was measured by the ^{1}H residual dipolar couplings encoded in the double-quantum (DQ) NMR build-up curves. The macroscopic properties such as those measured by tensile tests are discussed. A correlation between segmental orientation, TPU composition, and macroscopic properties including also previously reported DSC and rebound resilience measurements [18] is presented.

2. Experimental methods

2.1. Sample description and preparation

The raw materials for the preparation of the TPUs were: MDI (4,4′-diphenylmethane-diisocianate) and 1,4-butanediol (BD), commercial grade purchased from Bayer. Monourethane-type mold release agent (Freudenberg Dichtungs-Schwingungstechnik K.G.) was used in a concentration of 0.5%. Difunctional polycaprolactones (PCL) with different number average molecular weights M_n were purchased from Solvay Interox. The types of PCL were: Capa 2125, 2205, and 2304 with number average molecular weights of 1250, 2000 and 3000 g/mol, respectively. All chemicals were used as received, without any pretreatment.

In block-copolymers the molecular chains are composed of SS originating from the polyol and HS originating from the diisocyanate and the chain extender. Ideally, the two segments are immiscible and phase separate during their formation. The soft segments form the continuous soft phase in which the hard phase is dispersed. The domain size of the hard phase depends on the length of the hard segments, which can be adjusted through the mass fraction of diisocyanate and chain extender in the formulation and through the molecular weight of the polyol.

Table 1
Composition of the TPU samples

Polyol	M_n	Mass fraction of hard phase			
		23%	36%	45%	54%
Capa 2125	1250	Sample 3	Sample 4	Sample 5	Sample 6
Capa 2205	2000	Sample 7	Sample 8	Sample 9	Sample 10
Capa 2304	3000	Sample 11	Sample 12	Sample 13	Sample 14

The 12 samples have been prepared using the prepolymer technique. The formulations were calculated in a way that the sizes and ratios of hard segments were varied to specific numbers (Table 1). In each row, HS grow in size from left to right as the mass fraction is increased while using the same polyol. In each column the mass fraction of HS is held constant as the size of the polyol is increased. This means that HS grow in size by the same rate as the polyol is increased in molecular weight from one step to the next, but their number is reduced, so that the total concentration of the hard phase is always the same. The interphase between hard and soft phase decreases as the domain size of the phases increases from top to bottom.

2.2. Tensile test measurements

The mechanical deformation behaviour of the thermoplastic polyurethane samples was characterized by uniaxial tensile testing. Tensile bars of 75 mm length, 4 mm width, and 2 mm thickness were cut from the injection-moulded plates, post-cured 24 h at 110 °C. The bars were strained at 23 °C and 50% air humidity at a crosshead speed of 200 mm/min. The initial force was of 0.5 N. The tensile testing experiments were performed on a Zwick/Roell Z020/SN3A.02S0 testing machine, according to the standard norms DIN 53504-S2.

The stress–strain curves measurements were made including the break point and, therefore, no duplicate measurements on the same sample are possible. Nevertheless, the stress–strain measurements of five different samples with the same chemical composition were made and appear to be fairly homogeneous in their mechanical properties.

2.3. ^{1}H transverse magnetization relaxation

Proton NMR transverse magnetization relaxation decays (T_2—relaxation decays) were measured on a Bruker Minispec NMR—mq20 spectrometer at a proton resonance frequency of 20 MHz. The duration of the applied pulses were 1.86 μs for the 90° pulse and 3.68 μs for the 180° pulse. The dead time of the spectrometer is 10 μs. The spectrometer was equipped with a BVT3000 variable temperature unit. The achieved temperature stability was ±0.1 °C. The NMR experiments were performed at 40 °C. The room temperature samples were equilibrated with the measuring temperature by keeping them inside the measuring device for 15 min prior to the measurement. All the measurements performed on one sample lasted 2.4 h.

The free induction decay (FID) was measured in order to record the fast part of the transverse magnetization relaxation decay that corresponds to the dipolar-encoded signal from the hard segments. The FID edited by a Hahn echo pulse sequence is detected. Moreover, a Hahn echo pulse sequence $90^{\circ}_{x}-t-180^{\circ}_{x}-t-$acqusition was used to record the long decay component of the magnetization decay corresponding to the soft segments. The amplitude $A(t)$ of Hahn echo is not sensitive to the inhomogeneities of the static magnetic field and chemical shielding interaction. By varying the pulse spacing from 15 to 3000 μs the amplitude of the Hahn-echo was recorded as a function of time.

The solid echo was use for the measurements of the relative contribution of the hard segments to the total intensity of FID. This quantity is important for the normalization of the DQ build up curves. The inter-pulse spacing was varied from 13 to 40 μs and the amplitude of the solid echo was recorded as a function of time. The procedure is described in detail by Litvinov et al. [13] (and references therein).

The effective relaxation times for the hard and soft segments as well as the relative fraction of the relaxation components were obtained using a linear combination of a Gaussian (for the rigid segments) and an exponential decay function (for the soft segments). This combination was statistically the most relevant fit function for the transverse magnetization $M(t)$ and is described by

$$M(t) = A_{\mathrm{S}}\exp\left\{-\left(\frac{t}{T_{2\mathrm{S}}}\right)^{2}\right\} + A_{\mathrm{L}}\exp\left\{-\frac{t}{T_{2\mathrm{L}}}\right\}, \quad (1)$$

where A_{S} and A_{L} are the amplitudes of the short and long decays characterized by the effective transverse relaxation times $T_{2\mathrm{S}}$ ($T_{2\mathrm{S}}$ corresponds to the short component of transverse magnetization relaxation) and $T_{2\mathrm{L}}$, respectively. The experimental data are fitted according to Eq. (1) using the Microcal Origin 6.0 software.

2.4. ^{1}H double-quantum NMR

Proton double-quantum NMR build-up curves NMR experiments were performed on the same low-field NMR spectrometer as the transverse magnetization relaxation measurements (see above). Even and odd order multiple-quantum build-up curves can be measured using the five-pulse sequence (Fig. 1) [7] (and references therein). The phase cycling scheme used for detection of the MQ coherences of the order $\pm 2p$ is described in Ref. [4]. The length of the 90° radio-frequency pulse was about 1.86 μs, and a 1 s recycle delay was used. The pulse sequence implemented on the Bruker Minispec had 180° refocusing pulses (of 3.68 μs length) in the middle of excitation and reconversion periods. The DQ evolution time and the z-filter delay were fixed to $t_1 = 20$ μs and $\tau_{\mathrm{f}} = 20$ μs, respectively (Fig. 1). The values of the residual second van Vleck moments are obtained from the experimental data based on the procedure presented in Section 3.3. All DQ NMR experiments were performed on TPU samples at 40 °C.

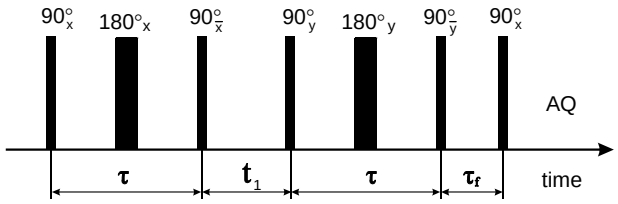

Fig. 1. Five-pulse sequence used for excitation of even-order multiple-quantum coherences. The reconversion period contains the same sequence of radio-frequency pulses with the phases orthogonal to the excitation pulses to generate a time-reversed dipolar double-quantum (DQ) Hamiltonian. The refocusing pulses of 180° are introduced in the middle of excitation and refocusing periods. For measurements of DQ build-up curves, the evolution of DQ coherences during the t_1 period is kept very short.

The measurements of the ^{1}H residual second van Vleck moments from the initial time regime of the DQ build-up curves need the normalization of the DQ filtered signals. This normalization employs the fraction of the hard phase measured from the transverse magnetization relaxation (Section 3.3).

3. Results and discussions

The microscopic and macroscopic properties of a series of thermoplastic polyurethane (TPU) samples with different content in hard segments and different molecular weight of the soft segments were recently investigated in Ref. [18]. Proton NMR transverse magnetization relaxation, DSC and rebound resilience techniques were used to characterize their molecular chain mobility, phase composition, glass transition temperatures and angles of rebound. The increase in the hard segments content at the same molecular weight soft segments leads to an increase in the glass transition temperature as determined by DSC and to a decrease in the angle of rebound as determined by rebound resilience. These quantities can be correlated to the decrease in the effective transverse relaxation rates of the soft segments and to the increase in the relative fraction of the hard segments as determined by NMR. By increasing the molecular weight of the soft segments at the same content of the hard segments the glass transition temperature and the angle of rebound decrease and the effective transverse relaxation times of the soft phase increase.

The studied TPU materials show multiple DSC endotherms between the glass transition of SS and the melting temperature of HS [18]. By comparing the endotherms of the samples with the same SS and increasing content of HS the melting peak maxima are shifted to higher values. This indicates both that SS influence the crystallinity of HS and also that more hydrogen bondings (through more HS) lead to higher structural stability. Moreover, the introduction of HS in a SS matrix shifts the glass transition temperature of pure SS towards higher values. The observed results were explained by a stronger interaction between soft and hard segments and a higher grade of miscibility of these two phases with increasing HS content and decreasing the molecular weight of SS. By keeping the content of HS constant, the increase in the molecular weight of SS leads to a decrease in their glass transition temperature T_{g}. This behavior is due to the longer SS chains, i.e. higher

molecular weight, which lead to a better phase separation within the material and thus to purer phases.

The DSC scans show small endotherms around 65 °C except for samples 12, 13, and 14 (36, 45 and 54% HS and 3000 g/mol polyol) which present these endotherms by less than 40 °C and samples 7 and 11 (23% HS and 2000 and 3000 g/mol $\bar{M}_n$ SS) which show melting points near 47 °C. All these thermal transitions are attributed to the melting of crystalline SS. Due to the low content of HS, the SS are comparatively pure and their melting temperature is close to the theoretical value (40 °C). For the other samples the melting peaks are 20 °C below and above the reported temperature. The reason for this behavior is the high molecular weight of the polyol used as SS, which makes the process of crystallization easier. However, with increasing HS the crystallinity of SS is reduced (see samples with 36% HS, 45% HS and 54% HS and 3000 g/mol $\bar{M}_n$ SS). For the rest of the samples the effect is opposite, the increase of the amount of HS leads to an increase in the melting peak of the crystalline SS. Here the broadness of the endotherm was taken into account. In the most cases the onset starts at 50 °C and goes on up to 80 °C and, hence, these endotherms include the melting of a mixture of crystalline SS and a very disordered mixed phase, containing hard and soft segments.

The melting peaks in the range 80–120 °C correspond to the mixed phase. The formation of the mixed phase is influenced by the block length, the block's incompatibility and by the composition. The mixed phase is a transition phase, from amorphous SS to crystalline or paracrystalline HS. Its structure is a mixture of amorphous and crystalline phase. All TPU samples presented an endotherm in this range.

For temperatures higher than 170 °C two endotherms are observed and are related to HS. One endotherm is in the range of 180–220 °C, and the other over 240 °C. The position of the peaks of the first range increases with increasing HS content. Moreover, the position of the peaks of the second range stays almost constant. For MDI/BD based HS in TPU's systems, paracrystalline and pure crystalline areas can be formed. In this case the first endotherm can be attributed to the paracrystalline HS and the second one to the pure crystalline HS. The change in the position of the peak maxima in each of the two cases supports this interpretation. No paracrystalline endotherm was observed for the samples 3, 4 and 7 (23% HS, 36% HS and 1250 g/mol SS and 23% HS and 2000 g/mol SS). Moreover, the samples 3, 7, 10, 11, 12 and 13 (23% HS and 1250 g/mol 54% HS and 2000 g/mol SS and 23, 36 and 45% HS and 3000 g/mol SS) do not present a pure crystalline HS endotherm.

3.1. Tensile test experiments

The superior mechanical properties of polyurethane are the result of the microphase separation of the hard and soft domains. The hard segments act as reinforcing filler in the soft segments matrix [19]. The relationship between the tensile properties of elastomers and their morphology was studied by Smith [20]. In general, the behaviour of a strained system depends on the size and the concentration of the hard segments, the ability of the segments to orient in the stretching direction, and the ability of the soft segments to crystallize under strain [21].

The stress–strain curves of the 2000 and 3000 g/mol SS series (samples 8–10 and samples 11–14 in Table 1) are shown in Fig. 2(a) and (b). Characteristic values derived from the stress–strain curves of all 12 samples are summarized in Table 2. Samples 3 and 7 are not discussed because the plates necessary to perform the tensile test could not be obtained, due to the low viscosity of the samples. According to Fig. 2, there are three regions to be discussed: first, the behaviour at low deformations, second the region of the plastic flow, and third the strain hardening region, at strains above 300%.

As seen in Fig. 2(b) the tensile properties are improving with increasing content of HS, at the same molecular weight of SS. Similar results are already reported in the literature [22,23]. The behaviour at low deformation (fewer than 5% strain) can be explained as the pure elastic deformation characteristic for regular elastomers [24]. Considering the sets of samples with the same molecular weight of SS, it is observed that with

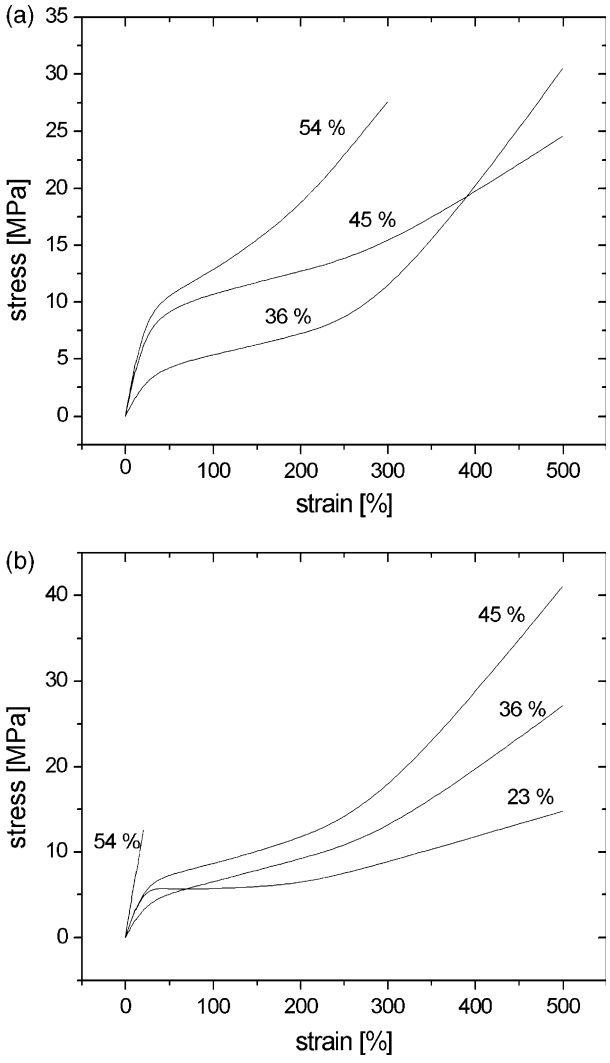

Fig. 2. Stress–strain curves of TPU materials in Table 1 with 2000 g/mol (a) and 3000 g/mol (b) molecular weight of the soft segments.

Table 2
Mechanical properties of TPU materials as determined by tensile tests

Sample	M_n (g/mol)	HS (%)	Yield stress (MPa)[a]	Yield strain (%)[a]	Young's module (MPa/mm^2)[a]	Stress at break (MPa)[a]	Strain at break (%)[a]
3	1250	23					
4	1250	36	7.44	4.95	6.68	23.00	554
5	1250	45	14.81	4.00	17.59	41.70	556
6	1250	54	18.92	1.60	55.97	42.20	520
7	2000	23					
8	2000	36	4.85	1.95	10.34	32.10	575
9	2000	45	8.96	1.7	25.65	39.30	580
10	2000	54	10.86	1.10	43.77	57.00	480
11	3000	23	9.81	1.25	44.33	29.50	629
12	3000	36	4.41	1.40	13.42	31.60	550
13	3000	45	6.33	0.90	32.75	47.60	571
14	3000	54	17.18	1.00	84.30	13.20	28

The values reported are average quantities over five measurements on different TPU samples.
[a] The errors are of the order ±3%.

increasing the HS content, Young's modulus given by the initial slope of the curves [25] also increases (Table 2). Fig. 3 shows a linear variation of the logarithm of the Young's modulus (E) with the content of HS [26], the increase in the crystallinity of the HS with increasing their content being a major factor which influences the Young's modulus.

The area of the plastic flow exhibits the same behaviour for all studied TPUs: the higher the HS content the higher the stress values when increasing the strain. It has already been proved that changes in the nature of the continuous phase of the material, from predominantly soft to hard, with increasing content of HS, contribute to the improvement of the tensile strength [22].

The dependence of the permanent deformation stress and strain on the content of HS is shown in Fig. 4. The yield point is difficult to define. It corresponds to the point, at which permanent plastic deformation starts [25], the point at which Hook's law is no longer valid [27]. The yield point depends on the type of material. It is directly related to the molecular mobility [27], and the accompanying stress depends on the crystallinity and the domain sizes of the rigid phase [28]. If the crystalline SS and the mixed phase are absent, the stress depends only on the content of HS and on the degree of segmental orientation. The increase in the content of HS leads then to an increase in the yield stress and to a decrease in

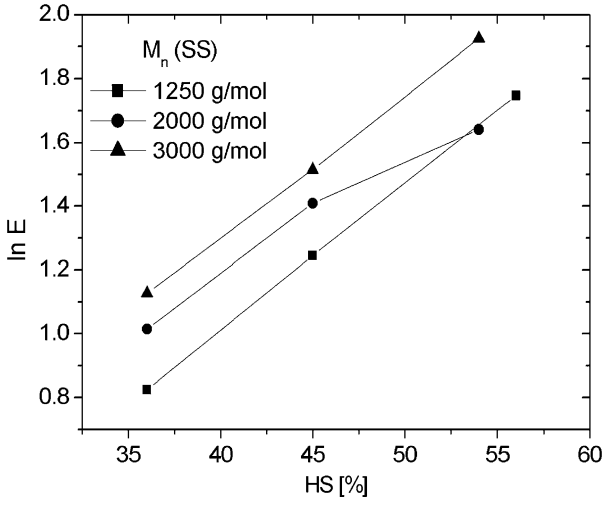

Fig. 3. Variation of the natural logarithm of Young's modulus as a function of the HS content (Tables 1 and 2).

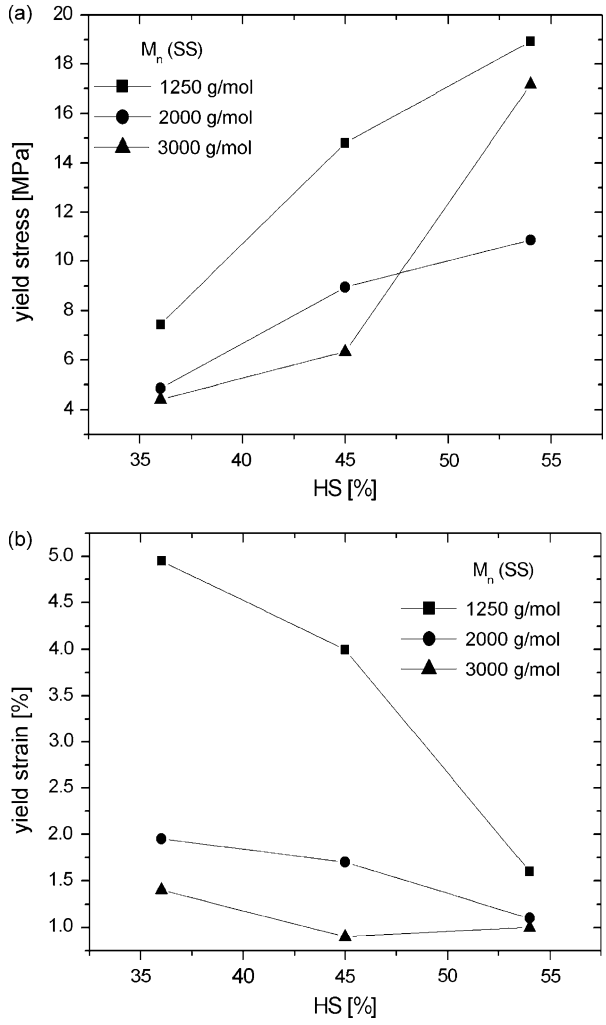

Fig. 4. Dependence of the yield stress (a) and the yield strain (b) as a function of the HS content (Table 2).

the strain at which the yield point occurs. This interpretation is consistent with the behaviour shown in Fig. 4.

Above 300% strain an upswing in some of the curves is observed. It is due to the strain-induced crystallisation of the chains of SS. For the 1250 g/mol molecular weight series this effect is not observed because the chains are too short to crystallize even under applied strain. In the 2000 g/mol series the stress–strain curves cross for the TPU samples with 36 and 45% content HS (Fig. 2(a)). According to DSC measurements [18] the T_g of the 36% HS sample is lower than that of the 45% HS sample. It implies a more pure SS phase, which can better crystallize under strain and which leads to a sudden increase in the tensile strength. On the other hand the DSC scans showed a higher melting heat at melt of crystalline SS in the 45% HS samples than in the 36% HS sample. This result proves that 45% HS sample is more crystalline in SS than the 36% HS sample. The melting range of crystalline SS is in both cases around 65 °C, so the degree of crystallinity should be similar in both cases. This explains the much higher stress necessary to deform the 45% HS sample up to 300% strain, compared to the 36% HS sample. At higher deformations, the already existent SS crystals in the 45% HS sample trigger the crystallization of the SS and leads to slower build of stress with increasing strain.

Sample 11 (23% HS and 3000 g/mol number average molecular weight) shows a behaviour different from all other samples over the entire stress–strain curve. Previous studies on the same TPU samples [18] show that sample 11 has well developed crystalline SS at room temperature. Together with the HS they oppose resistance to low deformation, an effect reflected in the high values of the stress at low strain. With increasing the stress, the crystalline SS are destroyed, and the sample cross-section decreases more rapidly at one particular point along the gauge length as a neck starts to form. The nominal stress starts to fall and settles at a constant value as the neck extends along the specimen. When the whole specimen is necked, strain hardening occurs and the stress rises until fracture takes place [25].

Sample 14 (54% HS and 3000 g/mol number average molecular weight) is in a co-continuous phase, where the components are not disperse anymore but exhibit separated, well defined structures. Here the amount of HS is high and parts of SS are already crystallized. This explains the high stress at low deformation. Furthermore, the soft phase orient in the stress direction and exerts pressure on the hard segments in which induces cracks so that the material breaks at lower strain.

As seen in Table 2, the stress at break increases with increasing content of HS, and the elongation at failure has a descending trend. The inhomogeneities in the materials, the degree of the phase separation, and the ability of the SS to crystallize under strain are reasons for the small deviations from these tendencies. The Young's modulus and the yield point are strongly influenced by the molecular mobility and the crystallinity of the rigid phase. The large values of the yield stress and Young's modulus and the lower values of yield strain can be correlated with an increased content of HS (at constant SS molecular weight) or block-length (at constant HS content) [21].

3.2. Effective ^1H transverse magnetization relaxation rates of hard segments

Effective ^{1}H transverse magnetization relaxation rates were acquired for the hard segments of the TPU series by the free induction decay edited by the Hahn echo. The experimental data were fitted by Eq. (1) to extract the effective relaxation rates $1/T_{2S}$. A Gaussian time dependence of the decaying NMR signals is assumed for the transverse relaxation of HS. Even if the fits based on this assumption are good this is not fully justified for the hard segments of TPU samples. The segmental motion of the hard segments, the presence of soft segments, and measuring temperature of 40 °C partially validates the Gaussian assumption. Moreover, $1/T_{2S}$ contains contribution from the crystalline SS and from the mixed phase, both of which exhibit larger segmental mobilities than the pure hard phase. This explains why the values of effective relaxation rates of HS measured at 40 °C (Table 3) are close to the ones of the SS measured at the same temperature and low compared to the ones of HS measured at 150 °C (not shown). For sample, 3 in Table 3 no HS were detected by NMR. Furthermore, by raising the measurement temperature up to 150 °C, sample 5 becomes a material with low viscosity. DSC data support the NMR results. Thus, the crystalline SS and the mixed phase seen by DSC seem to give a contribution only in the soft phase, the effective relaxation rates of which are increased.

The quantity $1/T_{2S}$ is directly related to the residual second van Vleck moment $\langle M_2 \rangle$. For a Gaussian line shape this relation is [7]

$$\frac{1}{T_{2S}} = \left(\frac{\langle M_2 \rangle}{2}\right)^{1/2} \tag{2}$$

The quantities $1/T_{2S}$ and $\langle M_2 \rangle$ are measured in separate experiments and, therefore, the validity of the Gaussian approximation can be verified (see below).

The dependence of the effective relaxation rates $1/T_{2S}$ on the content of hard segments for different values of the molecular weights of the soft segments in the TPU samples are shown in

Table 3
Amounts of the hard and soft segments and their ^{1}H effective transverse relaxation rates

Sample	M_n (g/mol)	HS (%)	A_S (%)[a]	$1/T_{2S}$ (m s^{-1})[a]	A_L (%)[a]	$1/T_{2L}$ (m s^{-1})[a,b]
3	1250	23	0	0	100	2.1
4	1250	36	28	14.1	72	3.4
5	1250	45	46	16.5	54	3.8
6	1250	54	66	18.2	36	4.7
7	2000	23	15	3.4	85	1.9
8	2000	36	28	7.1	72	2.9
9	2000	45	45	8.0	55	3.1
10	2000	54	58	9.3	42	3.9
11	3000	23	26	3.9	74	2.3
12	3000	36	30	4.0	70	2.5
13	3000	45	42	5.4	58	2.9
14	3000	54	57	6.1	43	2.2

[a] The errors are of the order ±5%.
[b] Reported in Ref. [18].

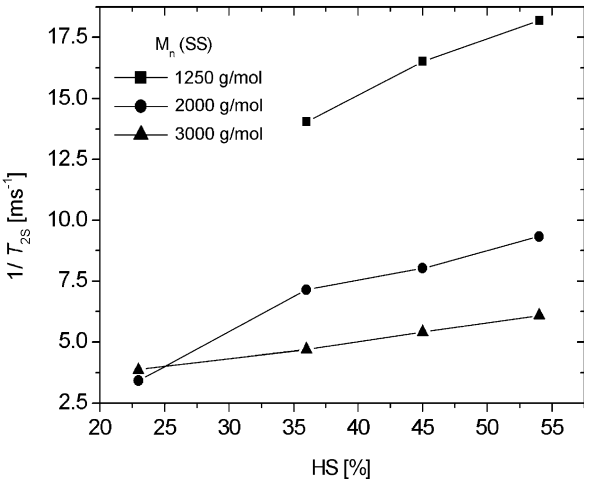

Fig. 5. Values of the ^{1}H effective transverse magnetization relaxation rates $1/T_{2S}$ of the hard segments in the TPU samples with the compositions shown in Table 1 as a function of the content in hard segments for different molecular weights of soft segments.

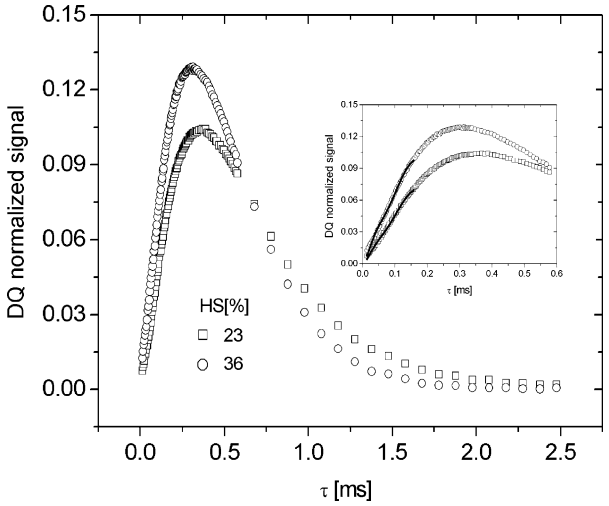

Fig. 6. Proton normalized double-quantum filtered signals for the TPU samples with 23% (squares) and 36% (circles) hard segments and the molecular weight of soft segments of 2000 g/mol as a function of the excitation/reconversion times τ (Fig. 2).

Fig. 5. The values of the quantities $1/T_{2S}$ increase almost linearly with the content of hard segments. This can be explained by an increase in the ^{1}H residual dipolar coupling strengths due to the reduction of the segmental mobility and an increase in the degree of ordering and packing of the segments in the hard phase. Fig. 5 shows also that the residual dipolar couplings of HS become smaller, i.e. the relaxation rates $1/T_{2S}$ decrease when the molecular weights of the soft segments increase. The segmental mobility of the hard segments reflected in the values of $1/T_{2S}$ is affected by the chain mobility of the soft segments (see also below).

3.3. Segmental orientation of the hard segments from ^{1}H DQ NMR experiments

Normalized ^{1}H DQ build-up curves for two TPU samples with different content of the hard segments and same molecular mass of soft segments are shown in Fig. 6. The maxima are the result of an influence of the transverse relaxation of the single-quantum coherences during the excitation and reconversion periods of the pulse sequence of the intensity of the edited DQ coherences (Fig. 1). This pulse sequence excites also high-order of even-order multiple-quantum coherences. However, in the initial excitation/reconversion regime the intensity of these coherences is dominated by the DQ coherences. This regime is exploited for the measurements of the ^{1}H residual dipolar couplings encoded in the residual second van Vleck moments [7]. It is obvious from Fig. 6 that only one maximum is detected. This shows that the residual dipolar couplings of the hard segments are larger in the pure than in the mixed phase and soft segments. For TPU samples with a mixed phase, DQ build-up curves will edit not only the hard phase but also the polymer chains from the mixed phase in the intermediate and long time regimes. We use in our investigation only the initial part of the DQ build-up curve that corresponds to the hard segments.

The initial rise in the DQ signals (see inset of Fig. 6) can be described in good approximation by a polynomial function in τ^2 derived from initial principles in Ref. [7], i.e.

$$S_{DQ}(2\tau) \propto \left\{ \frac{\langle M_2 \rangle}{2}\tau^2 - \frac{\langle M_4^{DQ} \rangle}{4!}\tau^4 + \cdots \right\} \exp\left[-\left(\frac{2\tau}{T_{2S}} \right)^2 \right], \qquad (3)$$

where $S_{DQ}(2\tau)$ is the normalized DQ signal. The effective transverse relaxation time of the hard segments is denoted by T_{2S}. We shall note that the residual higher-order DQ moments $\langle M_{2n}^{DQ} \rangle$, $(n>1)$ in Eq. (2) differ from the classical van Vleck moments $\langle M_{2n} \rangle$, $(n>1)$ [7].

The fits of the DQ built-up curves by Eq. (3) are shown in the inset of Fig. 6. In order to improve the accuracy of $\langle M_2 \rangle$ the T_{2S} values used in the fits were taken from separate measurements of the transverse magnetization relaxation (Table 3).

The values of the residual van Vleck moments for the hard segments correlate not only with the local and cooperative segmental motions of this phase but also with the constraints imposed by the soft segments. The dependence of $\langle M_2 \rangle$ on the HS content is shown in Fig. 7 for three TPU samples with different SS molecular weights. An increase in the values of $\langle M_2 \rangle$ with the HS content is evident for a given SS molecular weight. This behaviour reflects a higher degree of segmental orientation of the hard segments with an associated increase in the domain sizes. The effect of the molecular weight of the soft segments is also evident from the data in Fig. 7. In the case of low values of $\langle M_2 \rangle$ the changes in the segmental orientation are only slightly affected by an increasing HS content (Fig. 7). This is not longer valid for the TPU samples with higher values of the residual second van Vleck moments.

The interdependence of the values of ^{1}H residual dipolar couplings measured by $\langle M_2 \rangle$ and the values of $(1/T_{2S})^2$ is presented in Fig. 8. From Eq. (2) the slope of the dependence of $\langle M_2 \rangle$ versus $(1/T_{2S})^2$ is equal with two. Nevertheless, for the concentrations of 36% in HS where a quasi-linear dependence is measured the slope is close to unity. The same behaviour is

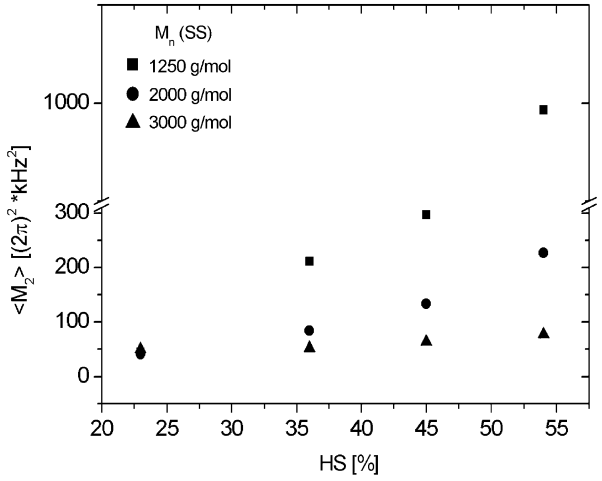

Fig. 7. Orientation of the hard segments measured from residual second van Vleck moment $\langle M_2 \rangle$ as a function of the HS content for different SS molecular weights (Table 1).

also valid for the other samples. Therefore, the Gaussian approximation is a poor approximation for the investigated TPU samples. This approximation affects mainly the effective values of $1/T_{2S}$ and it is not involved in the derivation of Eq. (3) for small values of the excitation/reconversion times, i.e. for $\tau < T_{2S}$. Nevertheless, the values of $\langle M_2 \rangle$ and $1/T_{2S}$ measured using Eqs. (1) and (3) will show the correct trend for the changes in the concentration of hard segments and number average molecular weights of soft segments.

3.4. Effect of the molecular weight of soft segments on $\langle M_2 \rangle$ of the hard segments

From the Figs. 5 and 7 it is evident that the values of $1/T_{2S}$ and $\langle M_2 \rangle$ decrease when the molecular weight of the soft segments increases. To explain qualitatively this effect a theoretical approach is given, based on the Rouse model of chain dynamics [29]. The theory shows that the soft segments produce constraints of the molecular dynamics in the hard

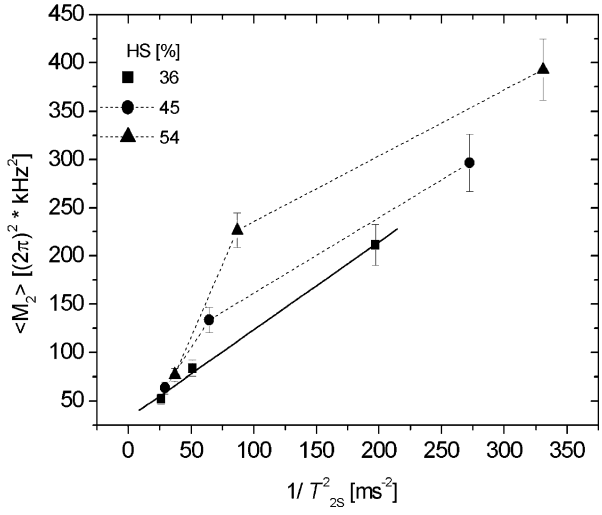

Fig. 8. Proton residual second van Vleck moments $\langle M_2 \rangle$ as a function of $(1/T_{2S})^2$ for the TPU series (Table 1). The straight line is a fit of the data for 36% HS.

segments that depends on the molecular weight M_n of the soft segments.

The instantaneous elongation $\vec{s}_n^m(t)$ of the Rouse modes m, of a segment n is given by [29]

$$\vec{s}_n^m(t) = \vec{s}_m \exp\left[\frac{i\pi n}{m}\right] \exp\left[-\frac{|t|}{\tau_m}\right], \tag{4}$$

where τ_m is the relaxation time of the Rouse mode m and $\vec{s}_m$ is the amplitude of oscillation of the mth Rouse mode. This mode involves relaxation on the scale of the chain sections with N/m monomers [30]. The quantity τ_m can be related to the number N of the monomers by

$$\tau_m \approx \tau_0 \left(\frac{N}{m}\right)^2, \tag{5}$$

where τ_0 is the relaxation time of a Kuhn monomer [30]. Therefore, from the above equation, we obtain $\tau_m \propto (M_n)^2$.

The instantaneous force present at the end of the sections with N/m monomers can be evaluated from the relationship: $\vec{F}_m(t) \propto M_n d^2\vec{s}_n^m(t)/dt^2$. The total force exerted by the soft segments on hard segments is given by $\langle \vec{F} \rangle_t \propto \langle \sum_m \vec{F}_m(t) \rangle_t$, where $\langle (\ldots) \rangle_t$ designates the time average. From the above equations we finally get $\langle F \rangle_t \propto (M_n)^{-1}$, i.e. the soft segments act on the hard segments with an average force inversely proportional to M_n.

The relationship between the average chain force and the values of $\langle M_2 \rangle$ and $1/T_{2S}$ of HS is difficult to be established. Nevertheless, it is evident from the above arguments that the values of $\langle M_2 \rangle$ and $1/T_{2S}$ will decrease as long as the molecular weight of soft segments increases. The soft segments with larger molecular weight will induce a less segmental orientation of the hard segments.

4. Microscopic–macroscopic properties correlations

The correlations between the segmental orientation as determined by the NMR measurements in terms of the residual dipolar coupling and Young's modulus, yielding stress, and strain determined from tensile testing of materials are shown in Fig. 9(a) and (b), respectively. With increasing amounts of HS for the same SS molecular weight, the Young's modulus and the yielding stress increase (Table 2), and the mobility of the rigid phase decreases leading to higher values of the residual van Vleck moments. This behavior is consistent with the existence of the hydrogen bridges whose amount increase with the content of HS, and which lead to more cohesive hard domains [21].

Fig. 9(c) shows that the yielding strains increase and the relaxation rates $(1/T_{2L})$ of SS reported in Ref. [18] (see also Table 3) decrease when the content of HS decreases and the molecular weight of SS increase. To explain the dependences shown in Fig. 9(c) two effects have to be taken into account: the influence of the HS on the mobility of SS through their amount, the degree of phase separation, and SS crystallinity that increases with their chain length. The amorphous SS are responsible for the elastic deformations. Under different

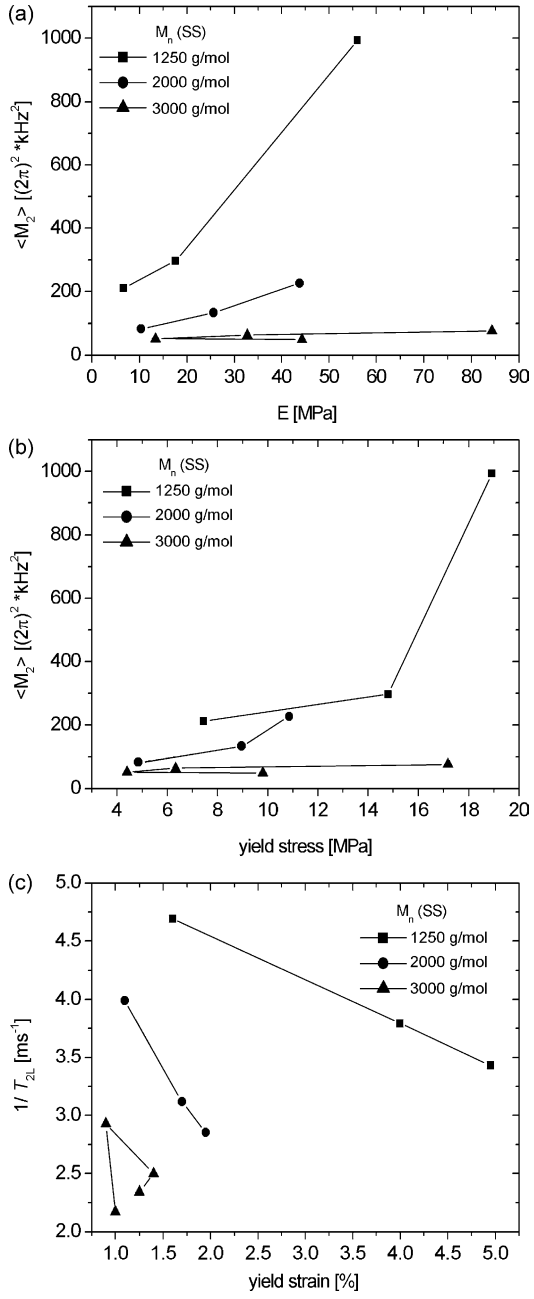

Fig. 9. Correlations of the HS segmental orientation in terms of residual van Vleck moments $\langle M_2 \rangle$ and the Young modulus (E) (a) and the yield stress (b) for the TPU samples (Table 1). The correlation between the transverse relaxation rates $1/T_{2L}$ of the soft segments [18] and yield stresses is shown in (c).

constraints, for instance, the presence of HS or crystalline SS, which reduces the free volume, their ability to expand is limited. In order to increase their free volume that will allow the material to reach a higher elastic behaviour, they force the limit to HS, to which they are directly connected. The structure of HS will be thus modified and the material undergoes plastic deformation.

A different behavior as the one discussed above, seems to have samples 11 and 14 in Fig. 9. Sample 11, as already discussed has better structured crystalline SS, which helps to improve the mechanical properties but is not sufficient to reduce the molecular mobility of SS. As already proved the high mobility of SS contributes, to the averaging of the residual dipolar coupling. Sample 14 is in a co-continuous phase with a high degree of phase separation, which explains the high mobility of SS as seen by NMR [18] but at the same time, this situation leads to enhanced mechanical properties as explained in Section 3.1.

The reason for establishing the correlation above is that during tensile testing the microstructure of the TPU samples changes. The extent of this change depends on the amount and length of hard and soft segments, two factors which influence the phase separation and the ability of SS to crystallize under strain. Until the material reaches the yielding point the changes are reversible. Under 5% strain the deformation is purely elastic. Under these circumstances the molecular mobility of these materials before testing, as well as the amount of the rigid phase should influence the Young's modulus and the yielding point of the tested material.

Proton residual second van Vleck moments become larger with decreasing HS mobility and can be can be correlated to the glass transition temperatures of the studied TPU samples taken from Ref. [18] (Fig. 10). The larger the chain mobility, the more averaged are the local dipolar fields which lead to lower values of $\langle M_2 \rangle$. At the same time higher chain mobility implies more free volume of the polymer, which will leads to lower values of the glass transition temperatures [31,32]. With increasing SS molecular weight (for the same amount of HS) the values of $\langle M_2 \rangle$ decrease. Moreover, longer soft chains lower the glass transition temperature of TPU samples [18].

The interaction between the hard and soft segments through their mutual influence on the chain mobility is another reason why the residual dipolar couplings of HS decrease when the HS content is decreased. The same dependence is also reflected by the angle of rebound as seen from the rebound resilience measurements [18] (Fig. 11). The more mobile the chains, the more averaged are the dipolar couplings and the more elastic is the material. By increasing the SS molecular weight at the

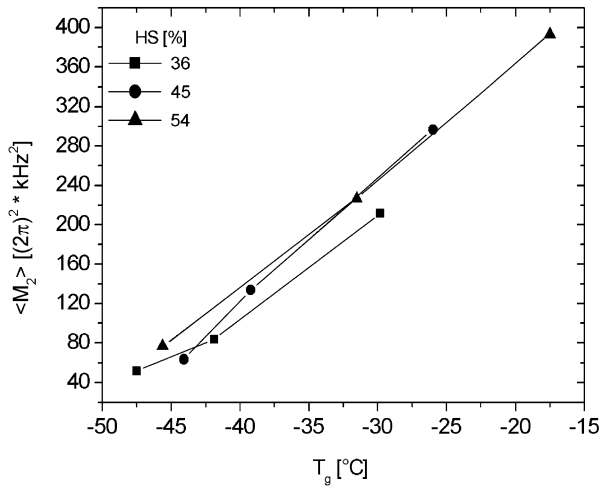

Fig. 10. Correlations of the HS segmental orientation in terms of residual van Vleck moments $\langle M_2 \rangle$ and the glass transition temperature (T_g) obtained from DSC measurements [18] for the TPU samples (Table 1).

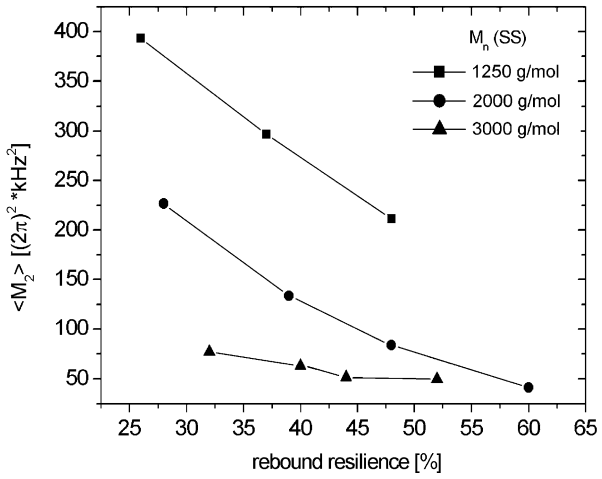

Fig. 11. Correlations of the HS segmental orientation in terms of residual van Vleck moments $\langle M_2 \rangle$ and the rebound resilience measurements described by the angle of rebound [18] for the TPU samples (Table 1).

same HS content, the dipolar coupling is better averaged through a higher SS mobility, but the angle of rebound is reduced due to the influence of the crystalline SS.

5. Conclusions

For the first time segmental orientation of the hard segments in thermoplastic urethane samples with different compositions was measured in terms of ^{1}H residual second van Vleck moments. These were measured model free from double-quantum build-up curves in the initial excitation/reconversion regime. The same information can be obtained in separate experiments from the effective transverse relaxation rates of the hard segments. Segmental orientation proves to be dependent on the content of the hard segments and the number average molecular weight of the soft segments. The value of the ^{1}H residual van Vleck moments increases when the content of the hard phase increases. A qualitative theoretical model was proposed to explain the dependence of $\langle M_2 \rangle$ on the molecular weight of the soft component in TPU samples. When the molecular weight of the SS increases the average stretching forces on the hard segments decreases and the segmental orientation of the hard phase is less pronounced.

The mechanical parameters like Young's modulus, yield stress and strain, and stress and strain at break were measured for TPU samples with the composition shown in Table 1. All these quantities depend on the composition of the TPU samples.

The segmental orientation of the hard phase is correlated with the mechanical quantities measured in tensile tests and rebound resilience measurements. Increasing the amount of HS for the same molecular weight of SS, Young's modulus, the yielding stress, and the residual dipolar coupling of the rigid phase increase as well. The yield strain increases, and the ^{1}H magnetization relaxation rates of SS decrease with decreasing HS content, and decrease with increasing SS molecular weight. These dependences can be explained inter alia by the changes in the phase composition that modifies the effective cross-linking of the soft chains and by partial crystallization of the soft phase. Moreover, by using the results of previous investigations of the same materials [18], the residual second van Vleck moments can be shown to correlate with the glass transition temperatures. A variation of the SS molecular weight for the same HS content leads to a decrease in the segmental orientation as well as of the glass transition temperature as determined by DSC [18].

A coherent and rational strategy for quality control of TPU materials can be developed based on the established correlation between sample compositions and microscopic and macroscopic parameters. The NMR measurements are non-destructive and were made with a low-field, low cost NMR spectrometer.

Acknowledgements

We are grateful to Mr R. Noll and Mr A. Rieder for the help with the hardness and tensile testing measurements. Alexandra Voda acknowledges Freudenberg Forschungsdienste KG (Physical Testing Department) for the financial support of her PhD work.

References

[1] Cohen Addad JP. Prog NMR Spectrosc 1993;25:1–312.
[2] Demco DE, Hafner S, Spiess HW. In: Litvinov VM, De PP, editors. Handbook of spectroscopy of rubbery materials. Shawbury: Rapra Technology Ltd; 2002.
[3] Demco DE, Blümich B. Encycl Polym Sci Technol 2004;10:637–85.
[4] Schneider M, Gasper L, Demco DE, Blümich B. J Chem Phys 1999;111:402–15.
[5] Fechete R, Demco DE, Blümich B. Macromolecules 2002;35:6083–5.
[6] Wang M, Bertmer M, Demco DE, Blümich B, Litvinov VM, Barthel H. Macromolecules 2003;36:4411–3.
[7] Voda M, Demco DE, Perlo J, Orza RA, Blümich B. J Magn Reson 2005;172:98–109.
[8] Maxwell RS, Balazs B. J Chem Phys 2002;116:10492–502.
[9] Saalwächter K, Ziegler P, Spyckerelle O, Haidar B, Vidal A, Sommer J-U. J Chem Phys 2003;116:3468–78.
[10] Saalwächter K. J Am Chem Soc 2003;125:14684–5.
[11] Wiesmath A, Filip C, Demco DE, Blümich B. J Magn Reson 2001;149:258–63.
[12] Wiesmath A, Filip C, Demco DE, Blümich B. J Magn Reson 2002;154:60–72.
[13] Litinov VM, Bertmer M, Gasper L, Demco DE, Blümich B. Macromolecules 2003;36:7598–606.
[14] Bertmer M, Gasper L, Demco DE, Blümich B, Litvinov VM. Macromol Chem Phys 2004;205:83–94.
[15] Hsu T-F, Lee Y-D. Polymer 1999;40:577–87.
[16] Kretschmer A, Drake R, Neidhoefer M, Wilhelm M. Solid State Nucl Magn Reson 2002;22:204–17.
[17] Idiyatullin DSh, Khozina EV, Smirnov VS. Solid State Nucl Magn Reson 1996;7:17–26.
[18] Voda A, Beck K, Schauber T, Adler M, Dabisch T, Bescher M, et al. Polym Test. In press.
[19] Show MC, DeSalvo GJ. On the plastic flow beneath a blunt axisymmetric intender. Trans ASME 1970;92.
[20] Smith TL. J Polym Sci Phys 1974;12:1825–35.

[21] Lelah MD, Cooper SL. Polyurethanes in medicine. Boca Raton, FL: CRC Press; 1953.
[22] Gopakumar S, Paul CI, Gopinathan Nair MR. Mater Sci (Poland) 2005; 23:227–32.
[23] Story RF, Hoffmann CD. Polymer 1992;33:2807–16.
[24] West JC, Cooper SL. Science and technology of rubber. New York: Academic Press; 1978.
[25] Young RJ. Introduction to polymers. Cambridge: University Press; 1983.
[26] Wegner G. Termoplastic elastomers. 1st ed. Munich: Carl Hansen; 1987.
[27] Roylance D. Yield and plastic flow.: Massachusetts Institute of Technology, Department of Materials Science Engineering; 2002.
[28] Niesten MCEI, Gaymans RJ. Polymer 2001;42:6199–207.
[29] Doi M, Edwards SF. The theory of polymer dynamics. Oxford: Clarendon Press; 1986.
[30] Rubinstein M, Colby R. Polymer physics. Oxford: University Press; 2003.
[31] Gent A-N. Engineering with rubber. Munich: Carl Hanser; 1992.
[32] Tobolsky AV. Properties and structure of polymers. New York, USA: Wiley; 1960.